Inorganic Chemistry

Communication

pubs.acs.org/IC

Tuning the Dimensionality of Interpenetration in a Pair of Framework-Catenation Isomers To Achieve Selective Adsorption of CO_2 and Fluorescent Sensing of Metal Ions

Rongming Wang, Minghui Zhang, Xiaobin Liu, Liangliang Zhang,* Zixi Kang, Wen Wang, Xiaoqing Wang, Fangna Dai, and Daofeng Sun*

State Key Laboratory of Heavy Oil Processing, College of Science, China University of Petroleum (East China), Qingdao, Shandong 266580, People's Republic of China

Supporting Information

ABSTRACT: A pair of framework-catenation isomers (**UPC-19** and **UPC-20**) based on an anthracene-functionality dicarboxylate ligand were synthesized and characterized for the first time through tuning of the dimensionality of interpenetration. The interpenetration dimensionality significantly influences the properties including the porosity, gas-uptake capacity, and fluorescent sensing ability: **UPC-19** with 5-fold interpenetration is nonporous, whereas the 3-fold interpenetration form of **UPC-20** is porous and exhibits selective adsorption of CO_2 and fluorescent sensing of Cu^{2+} and Fe^{3+} through fluorescence quenching.

Selective adsorption of CO_2 from flue gas using porous materials through physisorption is one of the most efficient and low-cost strategies to prevent global warming.[1] Currently, the widely used porous materials include zeolites, active carbons, and nanotubes.[2] Although some of these porous materials exhibit high stability and gas-uptake capacity, the low selectivity to CO_2 is the insuperable drawback for these materials in the application of CO_2 capture. Hence, developing new porous materials with high selectivity and gas-uptake capacity to CO_2 is still an extremely challenging task.

Metal−organic frameworks (MOFs) are a new type of porous material that is built from metal-based nodes and organic linkers and possesses potential applications in gas storage, catalysis, electronics, and drug delivery.[3,4] Recently, the studies of porous MOFs on the application of selective adsorption/capture have been increasing year by year.[5,6] On the basis of current research, one of the strategies to build porous MOFs with selective adsorption of CO_2 is to use the interpenetration nature of the frameworks, through which the pore size and geometry can be fully tuned and decorated to meet the requiring character for selective adsorption of CO_2.[7] Actually, interpenetration is a very common phenomenon in the construction of porous MOFs. In some cases, the generation of interpenetration in MOFs can significantly reduce the porosity to result in the formation of a nonporous framework,[8] although the single framework exhibits large channels. Hence, research on the control of interpenetration or tuning of the interpenetration dimensionality is very important for the construction of porous MOFs. In the past decade, several strategies such as applying rigid-rod-shaped secondary building units (SBUs), reducing reagent concentrations, using liquid-phase epitaxy, and introducing template molecules were successfully applied in the control of interpenetration in MOFs.[9,10] Recently, Hupp and our group reported a strategy that used organic ligand with hindrance groups to suppress the formation of interpenetrating frameworks.[11] Because the interpenetrating and noninterpenetrating frameworks showed quite different structural features, the control of interpenetration or tuning of the dimensionality of interpenetration in MOFs could generate porous MOF materials that exhibit unexpected properties including gas adsorption/separation, catalysis, and fluorescent sensor. However, studies on the tuning of the dimensionality of interpenetration in MOFs are seldom reported to date.[12] In this Communication, we report a pair of framework-catenation isomers, $Zn_4O(L^{OMe})_3$ (**UPC-19**) and $Zn_4O(L^{OMe})_3{\cdot}7H_2O$ (**UPC-20**), with different dimensionalities of interpenetration (Scheme 1). Furthermore, the isomer showed different gas-absorption and fluorescent-sensing properties.

Scheme 1. Schematic Representation of H_2L^{OMe} and Formation of Two Interpenetration Frameworks with Different Dimensionalities Controlled by the Temperature and Solvents

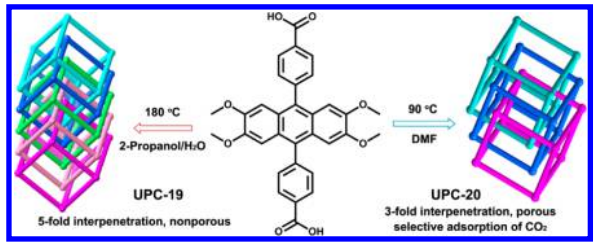

UPC-19 possesses a 5-fold interpenetrating framework with a pcu net, which is similar to the well-known MOF-5 series.[13] The $Zn_4O(COO)_6$ SBUs generated from the linkage of six carboxylate groups are connected by L^{OMe} ligands to generate an open framework with 3D channels (Figure S1a,b in the Supporting Information, SI). The dimensions of the channels are 19.2 × 11.9 Å. Because of the existence of large channels in the

Received: April 27, 2015
Published: June 18, 2015

DOI: 10.1021/acs.inorgchem.5b00934
Inorg. Chem. 2015, 54, 6084−6086

single net of **UPC-19**, five such nets interpenetrate mutually to provide a 3D dense structure with a 5-fold interpenetrating framework (Figure S1c in the SI). There are no obvious hydrogen-bonding or $\pi\cdots\pi$ interactions among the ligands in different nets.

UPC-20 exhibits a 3-fold interpenetrating framework based on a single net similar to that of **UPC-19**. Thus, **UPC-19** and **UPC-20** are a pair of framework-catenation isomers with different dimensionalities. In the crystal structure of **UPC-20**, there are two independent asymmetric units (A and B), forming two independent nets. As shown in Figure S2 in the SI, L^{OMe} ligands in A and B units are slightly distinct: the two benzene rings are almost vertical with the central anthracene ring, with average dihedral angles of 70.8° in unit A and 84.4° in unit B. The ligands in unit A link the $Zn_4O(COO)_6$ SBUs to generate a 3D open framework with a pcu net that is similar to the single net in **UPC-19**, whereas the ligands in unit B connect the $Zn_4O(COO)_6$ SBUs to give rise to a 3D framework that is different from the single net in **UPC-19**. Accordingly, two nets generated from unit A interpenetrate each other, providing a 2-fold interpenetrating framework, which further interpenetrates with the other net arising from unit B to result in the final 3-fold interpenetrating structure. The C−H$\cdots\pi$ interactions (3.79 Å) among the L^{OMe} ligands in different nets further stabilize the whole framework (Figure S3 in the SI). Despite the existence of interpenetration, **UPC-20** exhibits 1D channels along the [101] direction due to the low interpenetration dimensionality compared to that of **UPC-19**. After removal of guest solvents, a total solvent-accessible volume of 38.6% was calculated based on the *PLATON/VOID* routine for **UPC-20**.[14]

The porosities of the final frameworks in **UPC-19** and **UPC-20** were also investigated by gas-uptake measurements. As expected, a restricted adsorption behavior of **UPC-19** was observed for the N_2 adsorption isotherm at 77 K. A similar result was also found for CO_2 adsorption, as shown in Figure S4 in the SI, which is in agreement with the result from the crystal structure. In contrast, the N_2 adsorption isotherm at 77 K for **UPC-20** exhibits a reversible type I behavior, indicating its permanent porosity. The Brunauer−Emmett−Teller surface area calculated from the N_2 isotherm is 697.4 $m^2\ g^{-1}$, with a pore volume of 0.37 $cm^3\ g^{-1}$. Importantly, **UPC-20** can adsorb 42.7 $cm^3\ g^{-1}$ of CO_2 at 273 K, further confirming its porosity. In addition, various gas-uptake measurements including H_2 at 77 and 87 K, CO_2 at 295 K, and CH_4 and N_2 at 273 K were carried out for **UPC-20**. H_2 adsorption isotherms at 77 and 87 K also exhibit reversible type I behavior, with the largest amounts of adsorption being 91 and 64 $cm^3\ g^{-1}$, respectively. The corresponding heat of adsorption (*Qst*) for H_2 was calculated by fitting the H_2 adsorption isotherms at 77 and 87 K to a Virial-type expression. At the lowest coverage, *Qst* for H_2 was calculated to be ~5.4 kJ mol^{-1}, which is comparable to those of MOF-5 (4.7 kJ mol^{-1}) and MOF-177 (4.4 kJ mol^{-1}).[15] The CO_2 sorption measurements revealed that **UPC-20** can adsorb 42.7 and 22.3 $cm^3\ g^{-1}$ of CO_2 at 273 and 295 K, respectively, with a calculated *Qst* of 16.7 kJ mol^{-1}. The *Qst* value for CO_2 is comparable to that of Zn_4O(FMA) (16.1 kJ mol^{-1}),[16] which is the isoreticular structure with **UPC-20**.

However, **UPC-20** can only adsorb 9.4 $cm^3\ g^{-1}$ of CH_4 at 273 K, which may be due to the polar environment raised from the functionalized methoxy groups in the cavities of **UPC-20**. Accordingly, there is also no obvious adsorption of N_2 (only 2.9 $cm^3\ g^{-1}$) at 273 K. These results indicate that **UPC-20** can selectively adsorb CO_2 over N_2 and CH_4 at 273 K. To further confirm the performance of **UPC-20**, ideal adsorbed solution theory (IAST) was applied to evaluate the mixed-gas adsorption behavior. As shown in Figure 1, the selectivities of **UPC-20** for

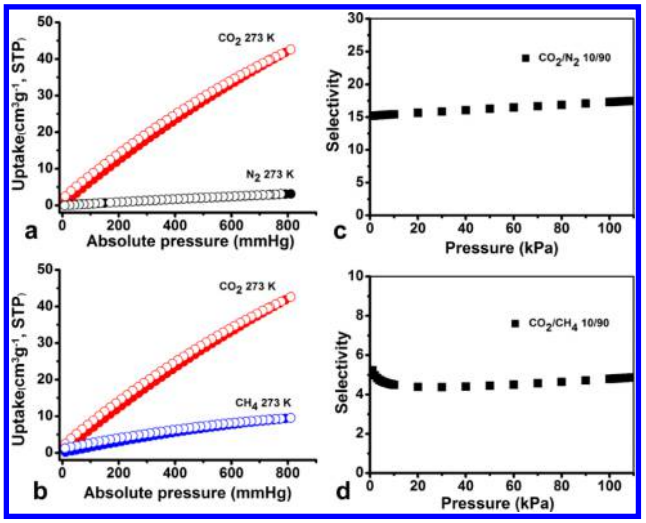

Figure 1. (a) CO_2/N_2 sorption isotherms at 273 K. (b) CO_2/CH_4 sorption at 273 K. (c and d) IAST CO_2/N_2 and CO_2/CH_4 selectivities for 10:90 CO_2/N_2 and CO_2/CH_4 mixtures, respectively, at 273 K.

CO_2 over CH_4 and N_2 under 10:90 CO_2/CH_4 and CO_2/N_2 gas mixtures are 5 and 15, respectively. In the past decade, although a large amount of literature reported control or tuning of the interpenetration in MOFs, achieving selective gas adsorption through tuning of the dimensionality of interpenetration in a pair of framework-catenation isomers remains unexplored prior to this work, to the best of our knowledge.

Another potential application for MOF materials is the fluorescent sensing of metal ions, organic molecules, etc., which have been widely studied in recent years.[17,18] Considering that the L^{OMe} ligand contains methoxy groups that can chelate metal ion,[19] the fluorescent sensing of metal ions was carried out for **UPC-19** and **UPC-20**. As expected, **UPC-19** and **UPC-20** showed quite different sensing abilities: **UPC-20** can selectively sense Cu^{2+} and Fe^{3+} ions through fluorescent quenching, whereas **UPC-19** cannot. In the measurement, we select dimethyl sulfoxide (DMSO) as the standard emulsion. The freshly prepared samples of **UPC-19** and **UPC-20** were ground and suspended in a DMSO solution, to which was added different metal ions dropwise in DMSO (1 mM). Interestingly, as shown in Figure 2, there is a slight effect on the luminescence intensity of **UPC-19** after the addition of Li^+, Ag^+, Cd^{2+}, Al^{3+}, Cu^{2+}, and Fe^{3+}. In contrast, the addition of Cu^{2+} and Fe^{3+} to the **UPC-20** emulsion can quench the luminescence significantly, indicating selective sensing of Cu^{2+} and Fe^{3+} through fluorescent quenching. The different sensing abilities to metal ions for **UPC-19** and **UPC-20** should derive from their structural features. As mentioned above, **UPC-19** is nonporous and thus metal ions cannot contact with the methoxy groups, whereas **UPC-20** is porous and metal ions can enter into the channels to interact with the methoxy groups.

In conclusion, a pair of framework-catenation isomers (**UPC-19** and **UPC-20**) was synthesized and characterized based on an anthracene-functionality dicarboxylate ligand and $Zn_4O(COO)_6$ SBUs with tuning of the interpenetration dimensionality, which is controlled by both the temperature and solvents used in the synthesis of the complexes. **UPC-19** with 5-fold interpenetration

DOI: 10.1021/acs.inorgchem.5b00934
Inorg. Chem. 2015, 54, 6084−6086

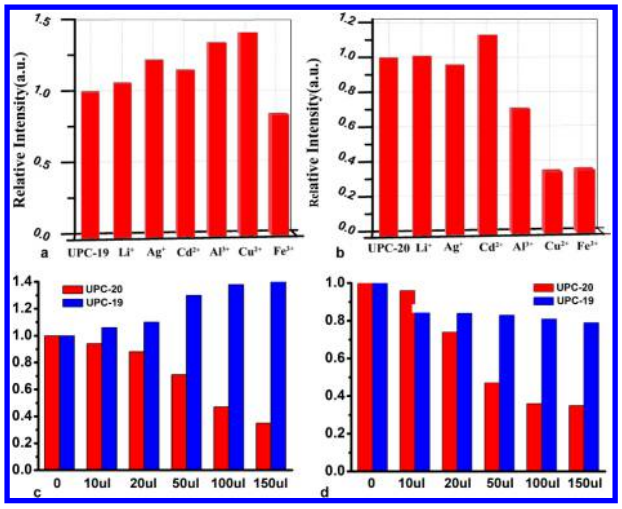

Figure 2. Photoluminescence intensities of **UPC-19** (a) and **UPC-20** (b) introduced into various metal ions and a comparison of the changes of the luminescent intensities for **UPC-19** and **UPC-20** after the gradual addition of Cu^{2+} (c) and Fe^{3+} (d) ions.

is nonporous, whereas **UPC-20** with 3-fold interpenetration is porous and exhibits selective adsorption of CO_2 over N_2 and CH_4 and fluorescence sensing of Cu^{2+} and Fe^{3+}. Although several strategies on the control of interpenetration in MOFs have been documented, to the best of our knowledge, this is the first report on achieving selective adsorption of CO_2 and selective sensing of metal ions through tuning of the interpenetration dimensionalities in a pair of isomers. Further studies will focus on the synthesis of a noninterpenetrating framework that is a single net in **UPC-19** and **UPC-20** by introducing template molecules and changing the solvents or reagent concentration.

■ ASSOCIATED CONTENT

Supporting Information

X-ray crystallographic data in CIF format, materials, methods and characterization, experimental section, and supplementary structure figures. The Supporting Information is available free of charge on the ACS Publications website at DOI: 10.1021/acs.inorgchem.5b00934.

■ AUTHOR INFORMATION

Corresponding Authors

*E-mail: liangliangzhang@upc.edu.cn.
*E-mail: dfsun@upc.edu.cn.

Notes

The authors declare no competing financial interest.

■ ACKNOWLEDGMENTS

This work was supported by the NSFC (Grants 21371179 and 21271117), Grant NCET-11-0309, the Shandong Natural Science Fund for Distinguished Young Scholars (Grant JQ201003), the Shandong Provincial Natural Science Foundation (Grant ZR2010BL011), and the Fundamental Research Funds for the Central Universities (Grants 13CX05010A, 14CX02150A, and 14CX02158A).

■ REFERENCES

(1) (a) Xiang, S. C.; He, Y. B.; Zhang, Z. J.; Wu, H.; Zhou, W.; Krishna, R.; Chen, B. L. *Nat. Commun.* **2012**, *3*, 954−963. (b) D'Alessandro, D. M.; Smit, B.; Long, J. R. *Angew. Chem., Int. Ed.* **2010**, *49*, 6058−6082.
(2) (a) Zhang, J.; Singh, R.; Webley, P. A. *Microporous Mesoporous Mater.* **2008**, *111*, 478−487. (b) Powell, C. E.; Qiao, G. G. *J. Membr. Sci.* **2006**, *279*, 1−49. (c) McEwen, J.; Hayman, J. D.; Yazaydin, A. O. *Chem. Phys.* **2013**, *412*, 72−76.
(3) For reviews, see: (a) Zhou, H. C.; Long, J. R.; Yaghi, O. M. *Chem. Rev.* **2012**, *112*, 673−674. (b) Ma, L.; Abney, C.; Lin, W. *Chem. Soc. Rev.* **2009**, *38*, 1248−1256. (c) Yoon, M.; Srirambalaji, R.; Kim, K. *Chem. Rev.* **2012**, *112*, 1196−1231. (d) Cui, Y. J.; Yue, Y. F.; Qian, G. D.; Chen, B. L. *Chem. Rev.* **2012**, *112*, 1126−1162.
(4) (a) Schoedel, A.; Boyette, W.; Wojtas, L.; Eddaoudi, M.; Zaworotko, M. J. *J. Am. Chem. Soc.* **2013**, *135*, 14016−14019. (b) Deria, P.; Mondloch, J. E.; Tylianakis, E.; Ghosh, P.; Bury, W.; Snurr, R. Q.; Hupp, J. T.; Farha, O. K. *J. Am. Chem. Soc.* **2013**, *135*, 16801−16804. (c) Du, L. T.; Lu, Z. Y.; Zheng, K. Y.; Wang, J. Y.; Zheng, X.; Pan, Y.; You, X. Z.; Bai, J. F. *J. Am. Chem. Soc.* **2013**, *135*, 562−565. (d) Zhang, M.; Feng, G. X.; Song, Z. G.; Zhou, Y. P.; Chao, H. Y.; Yuan, D. Q.; Tan, T. T. Y.; Guo, Z. G.; Hu, Z. G.; Tang, B. Z.; Liu, B.; Zhao, D. *J. Am. Chem. Soc.* **2014**, *136*, 7241−7244.
(5) (a) Li, J. R.; Sculley, J.; Zhou, H.-C. *Chem. Rev.* **2012**, *112*, 869−932. (b) Liu, J.; Thallapally, P. K.; McGrail, B. P.; Brown, D. R.; Liu, J. *Chem. Soc. Rev.* **2012**, *41*, 2308−2322.
(6) (a) Nugent, P. S.; Rhodus, V. L.; Pham, T.; Forrest, K.; Wojtas, L.; Space, B.; Zaworotko, M. J. *J. Am. Chem. Soc.* **2013**, *135*, 10950−10953. (b) Bloch, W. M.; Babarao, R.; Hill, M. R.; Doonan, C. J.; Sumby, C. J. *J. Am. Chem. Soc.* **2013**, *135*, 10441−10448. (c) Kong, L. D.; Zou, R. Y.; Bi, W. Z.; Zhong, R. Q.; Mu, W. J.; Liu, J.; Han, R. P. S. R.; Zou, Q. *J. Mater. Chem. A* **2014**, *2*, 17771−17778. (d) Lin, Q. P.; Wu, T.; Zheng, S. T.; Bu, X. H.; Feng, P. Y. *J. Am. Chem. Soc.* **2012**, *134*, 784−787.
(7) (a) Cheon, Y. E.; Park, J.; Suh, M. P. *Chem. Commun.* **2009**, 5436−5438. (b) Chen, B.; Ma, S.; Hurtado, E. J.; Lobkovsky, E. B.; Zhou, H.-C. *Inorg. Chem.* **2007**, *46*, 8490−8492.
(8) Zhao, X. L.; He, H. Y.; Hu, T. P.; Dai, F. N.; Sun, D. F. *Inorg. Chem.* **2009**, *48*, 8057−8059.
(9) (a) Rosi, N. L.; Kim, J.; Eddaoudi, M.; Chen, B. L.; O'Keeffe, M.; Yaghi, O. M. *J. Am. Chem. Soc.* **2005**, *127*, 1504−1518. (b) Tanaka, D.; Kitagawa, S. *Chem. Mater.* **2008**, *20*, 922−931.
(10) (a) Ma, S. Q.; Sun, D. F.; Ambrogio, M.; Fillinger, J. A.; Parkin, S.; Zhou, H. C. *J. Am. Chem. Soc.* **2007**, *129*, 1858−1859. (b) Ma, L. Q.; Lin, W. B. *J. Am. Chem. Soc.* **2008**, *130*, 13834−13835. (c) Zhang, J. J.; Wojtas, L.; Larsen, R. W.; Eddaoudi, M.; Zaworotko, M. J. *J. Am. Chem. Soc.* **2009**, *131*, 17040−17041.
(11) (a) Farha, O. K.; Malliakas, C. D.; Kanatzidis, M. G.; Hupp, J. T. *J. Am. Chem. Soc.* **2010**, *132*, 950−952. (b) He, H. Y.; Yuan, D. Q.; Ma, H. Q.; Sun, D. F.; Zhang, G. Q.; Zhou, H.-C. *Inorg. Chem.* **2010**, *49*, 7605−7607. (c) He, H. Y.; Ma, H. Q.; Sun, D.; Zhang, L. L.; Wang, R. M.; Sun, D. F. *Cryst. Growth Des.* **2013**, *13*, 3154−3161.
(12) Wang, Q.; Zhang, J. Y.; Zhuang, C. F.; Tang, Y.; Su, C. Y. *Inorg. Chem.* **2009**, *48*, 287−295.
(13) (a) Eddaoudi, M.; Kim, J.; Rosi, N. L.; Vodak, D. T.; Wachter, J.; O'Keeffe, M.; Yaghi, O. M. *Science* **2002**, *295*, 469−472. (b) Rowsell, J. L. C.; Yaghi, O. M. *Microporous Mesoporous Mater.* **2004**, *73*, 3−14.
(14) Spek, A. L. *J. Appl. Crystallogr.* **2003**, *36*, 7−13.
(15) (a) Furukawa, H.; Miller, M. A.; Yaghi, O. M. *J. Mater. Chem.* **2007**, *17*, 3197−3204. (b) Rowsell, J. C.; Yaghi, O. M. *J. Am. Chem. Soc.* **2006**, *128*, 1304−1315.
(16) Xue, M.; Liu, Y.; Schaffino, R. M.; Xiang, S.; Zhao, X.; Zhu, G.-S.; Qui, S.-L.; Chen, B. *Inorg. Chem.* **2009**, *48*, 4649−4651.
(17) (a) Cui, Y. J.; Yue, Y. F.; Qian, G. D.; Chen, B. L. *Chem. Rev.* **2012**, *112*, 1126−1162. (b) Hu, Z. C.; Deibert, B. J.; Li, J. *Chem. Soc. Rev.* **2014**, *43*, 5815−5840. (c) Kreno, L. E.; Leong, K.; Farha, O. K.; Allendorf, M.; Van Duyne, R. P.; Hupp, J. T. *Chem. Rev.* **2012**, *112*, 1105−1125.
(18) (a) Chen, B. L.; Wang, L.; Zapata, F.; Qian, G.; Lobkovsky, E. B. *J. Am. Chem. Soc.* **2008**, *130*, 6718−6719. (b) Chen, Z.; Sun, Y. W.; Zhang, L. L.; Sun, D.; Liu, F. L.; Meng, Q. G.; Wang, R. M.; Sun, D. F. *Chem. Commun.* **2013**, *49*, 11557−11559.
(19) Denmark, S. E.; Edwards, J. P.; Wilson, S. R. *J. Am. Chem. Soc.* **1991**, *113*, 723−725.

DOI: 10.1021/acs.inorgchem.5b00934
Inorg. Chem. 2015, 54, 6084−6086